Available online at www.sciencedirect.com
SCIENCE DIRECT
Polymer 46 (2005) 9863–9870
polymer
www.elsevier.com/locate/polymer

Preparation and properties of starch thermoplastics modified with waterborne polyurethane from renewable resources

Yongshang Lu[a], Lan Tighzert[a,*], Patrice Dole[b], Damien Erre[c]

[a]*Centre d' Etudes et de Recherche en Matériaux et Emballage (CERME), Ecole Supérieure d'Ingénieurs en Emballage et Conditionnement (ESIEC), Esplanade Rolland Garros-Pôle Henri-Farman B.P.1029, 51686 Reims Cedex 2, France*
[b]*INRA UMR FARE, Equipe emballage, CPCB Moulin de la Housse BP 1039, 51687 Reims Cedex 2, France*
[c]*Laboratoire de Microscopies et d'Etude de Nanostructures (LMEN) EA3799, Université de Reims Champagne-Ardenne, 51687 Reims Cedex 2, France*

Received 4 February 2005; received in revised form 7 June 2005; accepted 9 August 2005
Available online 29 August 2005

Abstract

A waterborne polyurethane (PU) aqueous dispersion was synthesized from castor oil, and blended with thermoplastic starch (TPS) to obtain a novel biodegradable plastic with improved physical properties. The effect of PU content on the morphology, miscibility and physical properties of the resulting blends was well investigated by scanning electron microscopy, differential scanning calorimetry, dynamic mechanical thermal analysis and measurements of mechanical properties and water sensitivity. The research results show that the blends exhibit a higher miscibility when PU content is lower than 15 wt% due to the hydrogen bonding interaction between urethane groups and hydroxyl groups on starch, whereas obviously phase separation occurs in the blends with more than 15 wt% PU. Incorporating PU of 4–20 wt% in TPS results in the blends with improved Young's modulus (40–75 MPa), tensile strength (3.4–5.1 MPa), elongation at break (116–176%). Further, PU also plays an important role in improving the surface- and bulk-hydrophobicity and water resistance of the resulting blends.

Keywords: Thermoplastic starch; Polyurethane; Castor oil

1. Introduction

Worldwide potential demands for replacing petroleum derived raw materials by renewable resources in production of valuable biodegradable polymeric materials are quite significant from the social and environmental viewpoints [1,2]. However, up to the present, the biodegradable polymers cannot be used for wide applications because of their limitations in prices or properties. Among the several candidates including aliphatic polyesters, natural polymers and their derivatives, starch, a polysaccharide produced by many plants as a storage polymer, is one of the most promising materials for biodegradable plastics because it is easily available all over the world with a low price [3]. Native starch occurs in the form of discrete and partially crystalline microscopic granules that are held together by an extended micellar network of associated molecules [4], which make it difficult to melt or process. However, incorporating plastifying agents, such as glycerol and water, can lower the glass transition temperature and melting temperature of the starch. Thus, starch is suitable for thermoplastic processing to become an essentially homogeneous material called thermoplastic starch (TPS) [5]. Utilization of TPS for biodegradable plastics has received considerable attention during past two decades due to their renewability, low cost, easy availability, and easy modification chemically and mechanically [6]. Unfortunately, TPS by itself is a poor choice as a replacement for any plastics because of its poor mechanical properties and high water susceptibility [7]. Consequently, several strategies have been created to cope with these problems including modification of the starch structure [8,9], blends with other biodegradable polymers [10,11], compatibilizer use to enhance interfacial adhesion of starch, based blends [12,13], and reinforcer addition of fibrils [4,14], whiskers [15,16] and clays [17,18].

* Corresponding author. Tel./fax: +33 3 26 91 37 64.
E-mail address: lan.tighzert@univ-reims.fr (L. Tighzert).

0032-3861/$ - see front matter © 2005 Elsevier Ltd. All rights reserved.
doi:10.1016/j.polymer.2005.08.026

Polyurethane (PU), with properties covering from a high performance elastomer to tough thermoplastic, has been extensively used due to its excellent physical properties (e.g. high tensile strength, abrasion and tear resistance, oil and solvent resistance, low flexibility temperature, printability, etc.) and high versatility in chemical structures [19,20]. However, driven by continuous reduction in costs and the control of volatile organic compound emissions, the development of waterborne polyurethane or poly-(urethane–urea) formulations has been increasing [21]. The resulting water-borne polyurethanes present many advantages related to conventional solvent-borne ones such as low viscosity at high molecular weight and good applicability [22]. Environmental protection can be better realized when the polyol is replaced with renewable sources, such as some vegetable oils, to synthesize the water-borne urethane materials, although this kind of research work has not attracted much attention. Among many kinds of vegetable oils, the castor oil possessing three hydroxyl groups is a very good candidate for synthesis of water-borne polyurethane. Ha et al. [23] found that incorporating polyester based polyurethane into starch can, to some extent, enhance mechanical properties or water resistance of the resulting materials. Further, the partial miscible blends on whole composition ratio with improved physical properties could be prepared by mixing the aqueous dispersions of starch and polyester based waterborne polyurethane [24]. In view of both environmental conservation and sufficient utilization of renewable resources, we thus, in this work, attempted to use castor oil to synthesize a water-borne polyurethane, and then used it to modify the glycerol plasticized starch by extrusion processing in order to obtain economically viable biodegradable materials with enhanced properties. The morphology, miscibility, mechanical properties and water-resistance of the blends with different polyurethane content were well investigated and discussed.

2. Experimental section

2.1. Materials

Wheat starch was obtained from Chamtor (France). Residual protein content was less than 1 wt%. Castor oil (hydroxyl number, 163 mg KOH/g), glycerol (99.5% purity), isophorone diisocyanate (IPDI), dimethylol propionic acid (DMPA) and triethylamine (TEA) were purchased from Aldrich and used as received without further purification.

2.2. Preparation of polyurethane dispersion based on castor oil

Castor oil (34.5 g), IPDI (22.2 g), and DMPA (5.4 g) were charged into a four-necked flask equipped with mechanical stirrer, nitrogen inlet, condenser and thermometer. The reaction was carried out at 95 °C for 4 h under dry nitrogen atmosphere. Subsequently, the resulting prepolymer was cooled to about 40 °C and about 50 mL acetone was poured into the flask to reduce the viscosity. After neutralization of carboxylic groups of DMPA with TEA of 4.1 g for 30 min, the polyurethane containing 44 wt% hard segment was dispersed with distilled water to obtain 15 wt% waterborne polyurethane (PU) dispersion under vigorous stirring. After being stored in room temperature for a week, the PU dispersion was concentrated to 70 wt% solid content at 30 °C with a rotary vacuum-evaporator.

2.3. Extrusion processing

Prior to processing, desired weight of dried starch and glycerol were mixed for 10 min in a mixer and then left to stand 30 min at 140 °C, allowing penetration of glycerol into the starch granule. After cooling, the PU dispersion and desired distilled water were added and mixed for another 20 min. The total content of glycerol and water were controlled to form the formulation of starch: glycerol:water is 70:20:10. Finally, the mixtures were extruded into strand by using a laboratory-scale single screw extruder ($L/D = 11$, SCAMIA, France) equipped with a slit die. The temperature profile along the extruder barrel was controlled to be 105, 110 and 120 °C (from feed to die). The screw rotation speed was 40 rpm. To improve the compatibility between PU and TPS matrix, the extrudates were palletized and subsequently extruded into ribbons of about 30 mm × 0.4 mm (width × thickness) by a slit die. Extruder temperature control zones were set to 110/115/120/120 °C (feed to slit die). The screw rotation speed was 30 rpm. By changing PU content of 0, 4, 7, 10, 15, 20 and 30 wt% in TPS, a series of extrudates were obtained and coded as TPS, SP-4, SP-7, SP-10, SP-15, SP-20 and SP-30, respectively.

Before various characterizations, the extruded ribbons were conditioned at 52% relative humidity (RH) for at least 10 days at ambient temperature, in a closed chamber containing a $Mg(NO_3)_2 \cdot 6H_2O$ saturated solution of distilled water [25].

2.4. Characterizations

FT-IR spectrum of the polyurethane was recorded with a Nicolet Protégé 460 FT-IR spectrometer (Madison, USA) using KBr pellets.

The DSC analysis of TPS, PU and TPS/PU blends was performed using a differential scanning calorimeter (TA2920, USA). Samples (15–20 mg) were cut from extruded strands conditioned at 52% RH and analyzed. Each sample was subjected to the heating/cooling cycle between −50 and 100 °C to obtain reproducible the glass temperature (T_g) values. Scanning rate was 5 °C/min.

Dynamic mechanical behavior of the specimens, kept at a conditioning cabinet of 25 °C and 35% RH, were

determined with a dynamic mechanical thermal analyzer (TA instrument DMA 2980-USA) with tensile mode at 1 Hz with a strain of 30 μm and a heating rate of 5 °C/min in the temperature range from −90 to 100 °C. The specimens with typical size of 10 mm×0.5 mm (length×width) were used and coated with a thin layer of silicone wax to avoid water evaporation during scanning.

Morphology of the film cross-sections fractured under liquid nitrogen was investigated by an analysis scanning electron microscopy (JEOL JSM-6100LA).

The tensile strength, elongation at break and Young's Modulus of the blends were determined with a mechanical testing machine (Test 110 from GT Test, France), with a crosshead speed of 10 mm/min. The dumb-bell specimens of 17 mm×4 mm (length×width) were cut from the extruded ribbons directly using a dumbbell shape knife. The toughness of the polymer, which is the fracture energy per unit volume of the sample, was obtained from the area under the corresponding tensile stress–strain curve. An average value of at least eight replicates of each material was taken.

The contact angle measurements were performed with a Kruss G23 (Germany) apparatus. A water droplet was deposited on the sample surface and the droplet shape was recorded. A CCD video camera and image analysis software were used to determine the contact angle evolution. Results are the average values of quadruplicate.

The dried samples of 20 mm×10 mm, kept at 0% RH atmosphere over P_2O_5 in a desiccator for 1 week, were weighed and then conditioned at 25 °C in a chamber containing saturated solution of $CuSO_4 \cdot 5H_2O$ to ensure a 98% RH. The samples were removed at desired intervals and weighed until the equilibrium state was reached. The water uptake of the samples was calculated as follows:

$$\text{Water uptake } (\%) = \frac{W_t - W_0}{W_0} \times 100 \quad (1)$$

where W_t and W_0 are the weight of the sample at time t in 98% RH and the initial weight of the sample, respectively.

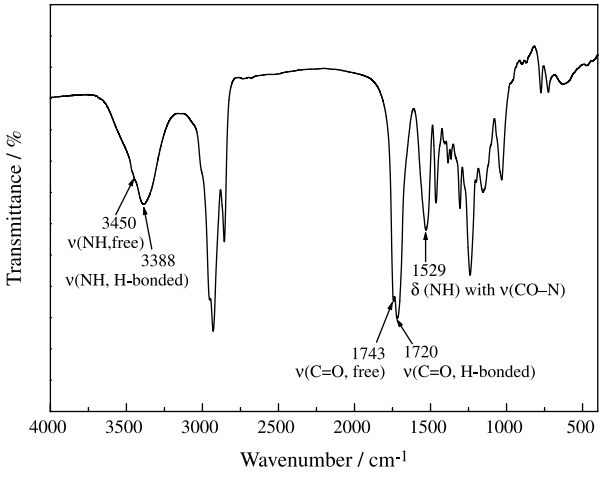

Fig. 1. FT-IR spectrum of waterborne polyurethane prepared from castor oil.

3. Results and discussions

3.1. Miscibility and morphology

Fig. 1 shows the FT-IR spectrum of castor oil based PU prepared from water dispersion. Peaks of the NH stretching band (νNH) of PU is observed at 3388 and 3450 cm^{-1}, which are assigned to the hydrogen-bonded NH groups (νNH, H-bonded) with urethane carbonyl groups and free one (νNH, free), respectively. The shoulder peak of free νNH indicates that most of NH groups in the polyurethane form the hydrogen bonding with carbonyl oxygen. The carbonyl stretching band region displays two peaks at 1743 and 1720 cm^{-1}, which can be, respectively, assigned to the stretching of the free carbonyl groups (νC=O, free) and hydrogen bonded one (νC=O, H-bond) [26]. The occurrence of these characteristic peaks of indicates good preparation of water-borne polyurethane derivated from castor oil.

The measurement of the glass transition temperature (T_g) of a polymer blend is often used as a criterion to determine its miscibility. A miscible polymer blend would exhibit a single transition between T_gs of the two components. With increasing immiscibility there is a broadening of the transition, whereas an incompatible system would be marked by separate transitions of the polymer components in the blends [27]. The DSC curves of TPS, PU and their blends are shown in Fig. 2, and the corresponding data of T_g are summarized in Table 1. The T_gs of PU and TPS are determined to be about 10.6 and 36.5 °C, respectively. Due to substantial differences in chemical structure of polyurethane compared to plasticized starch and relative large

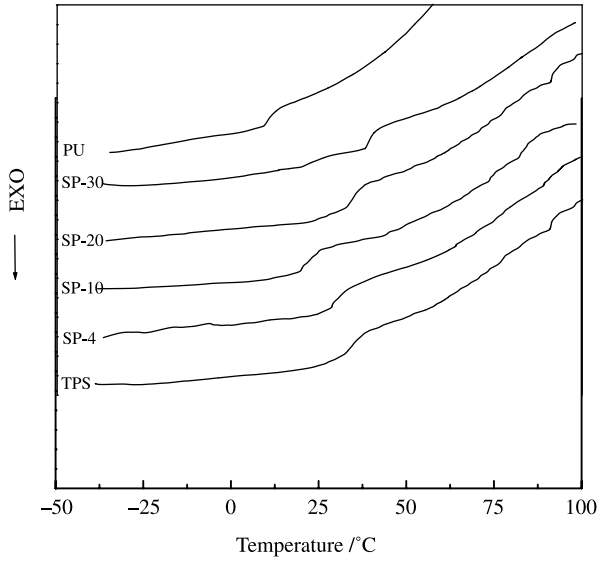

Fig. 2. DSC curves of TPS, PU and TPS/PU blends.

Table 1
Thermal analysis data for TPS, PU and the blends determined by DMTA and DSC

Samples	DMTA		DSC	
	T_{α_1} (°C)	T_{α_2} (°C)	T_g (°C)	ΔC_p (J g^{-1} K^{-1})
TPS	−42.2	75.8	35.2	0.44
SP-4	−41.7	72.2	30.7	0.40
SP-7	−41.4	63.9	32.3	0.15
SP-10	−34.6	38.6	20.1	0.13
SP-15	−39.3	52.3; 79.9	26.5	0.17
SP-20	−35.3	45.5; 85.9	27.5; 34.3	0.16; 0.26
SP-30	−36.5	56.1; 81.5	22.4, 39.7	0.089; 0.23
PU	–	29.8	10.5	0.548

DMTA and DSC were performed in 35 and 52% RH, respectively.

divergence in T_gs (>20 °C) make it possible to detect individual transition of two polymers by DSC [28]. For the blends with PU content less than 20 wt%, one single T_g is observed, which shifts from about 32.3 to 20.1 °C. This is an indication that the synergistic interaction occurs between TPS and PU, which leads to a higher miscibility between PU and TPS. As the PU content further increases, the blend exhibits two T_gs, corresponding to starch and PU, respectively. The observation of two T_gs is in good agreement with the visual opaque appearance of the blends containing higher PU content than 15 wt%, which suggests that the blends are heterogeneous and two starting components may fractionate in two different phases [28]. However, T_g transition at lower temperature is broadened and the divergence of two T_gs in the blends is reduced compared with that between pure TPS and PU. Further, the T_g corresponding to TPS in SP-30 is higher than that of pure TPS. This indicates that the hydrogen bonding interactions are taking place in the blends, leading to the mutual solubility between TPS and PU. This result will be confirmed further by DMTA characterization. However, these interactions are not strong enough to ensure the miscibility of the blends with high content of PU. A similar observation was also reported for the styrene-*co*-maleic anhydride random copolymers (SMA)/polyacrylates blends, which is immiscible when the content of maleic anhydride groups is lower than 8 wt% [29]. Compared with TPS and PU, the heat capacity change (ΔC_p) of the blends at T_g transition is reduced. This reduction seems too high with respect to the small quantity of PU introduced. Nevertheless, it could indicate a reduction in the number of the thermal activated starch chain units resulted from the intermolecular interactions between PU and TPS [30].

Dynamic mechanical thermal analysis is a valuable technique to investigate the mechanical behavior of materials subjected to cyclic stress and to obtain information about the relaxation mechanisms that may be correlated with the dynamics and the microstructure of the material [31]. Unfortunately, the relaxation peaks of PU and TPS, conditioned at 52% RH, are observed to be 28 and 35 °C (data not shown here), which differs only by 7 °C. This small difference in relaxation temperature (T_α) does not permit to distinguish definitely the transitions of TPS/PU blends. In order to distinguish the relaxation process of the component polymer in the blends, the specimens conditioned at 35% RH for 1 week, though which the T_α of TPS might shift to higher temperature, was used for DMTA investigation. TPS is more sensitive to humidity than PU, so the divergence between their T_gs increases when the humidity decreases from 52 to 35 RH%. The storage modulus (E') and loss angle tangent (tan δ) peaks versus temperature for TPS, PU and the blends are presented in Figs. 3 and 4, respectively. The storage moduli of TPS and the blends decrease very sharply in the temperature region of both −60 to −25 °C and 0 to 75 °C (Fig. 3). Such two-step decreases of the modulus for starchy material, reflecting a stiffness loss, were also reported by other authors [14,32]. According to Anglès et al. [14] and Lourdin et al. [32], the glycerol plasticized starch with the formulation used in this work exhibits as a heterogeneous system consisted of glycerol rich domains dispersed into the

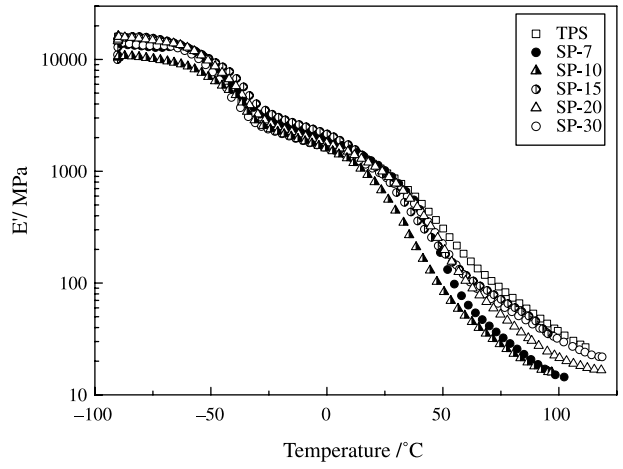

Fig. 3. Temperature dependence of storage modulus (E') for TPS and TPS/PU blends.

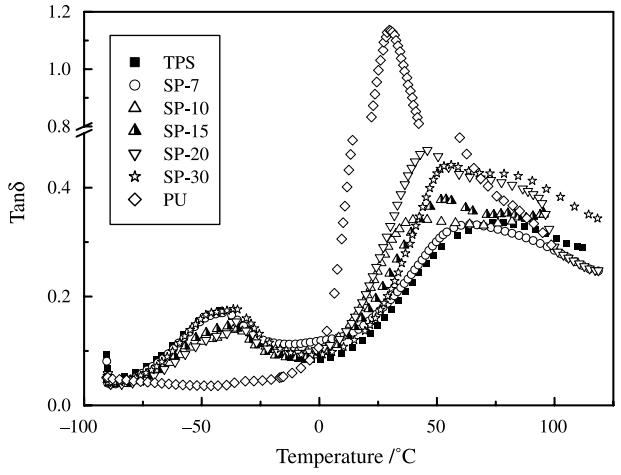

Fig. 4. Temperature dependence of mechanical loss factor (tan δ) for TPS, PU and TPS/PU blends.

starch-rich matrix. So the two-relaxation transitions occur: a high-temperature T_α intrinsic to a starch-rich phase and a low-temperature T_α intrinsic to the local motions of glycerol linked to starch hydroxyls. Two observed modulus drops are therefore ascribed to energy dissipation phenomena involving cooperative motions of long amorphous sequences likely to rotate and translate in different surroundings. The dropped moduli are expressed in the concomitant relaxation processes where the loss angle tangent ($\tan\delta$) passes through two successive maxima (Fig. 4), which corresponds to the T_α transition of the materials summarized in Table 1. The position, height and shape of $\tan\delta$ peak provide information about the degree of order and freedom of molecular mobility of the polymer chain segments [33]. In agreement with DSC results, the blends, containing less than 15 wt% PU, display one broad loss peak and its maximum shifts to lower temperature compared with that of TPS. This is an indication that some specific interactions are taking place between the polar groups of the TPS and PU, leading to a mutual solubility of the polymers with a concurrent change in T_α. However, the observation of two well-separated $\tan\delta$ peaks for SP-15 is in contradiction with the result from DSC, from which only one T_g transition is observed. Due to high sensitivity of DMTA technology and larger divergence in T_a (about 45 °C) between PU and TPS, for the SP-15 DMTA seems to give more conclusive results compared with DSC. As a consequence, the distinct PU domains begin to come into being in the blend of SP-15. With increasing PU content, SP-20 and SP-30 exhibit two obviously relaxation processes, one for each phase. Considering position and height of the loss peaks of these phase-separated blends, there are still some mutual solubility between TPS and PU, maybe in interfaces between each phase.

The morphology of the fractured surface of TPS and TPS/PU blends are shown in Fig. 5. TPS displays a homogenous morphology, implying that the granules of the starch are destroyed and form a homogeneous phase. The relatively smooth morphology, except for some edge resulted during being broken, is observed for the blend SP-7, indicating higher miscibility of the blends when PU content is relatively low. Further increasing PU content, the morphology of dispersed PU phase into TPS continuous phase occurs in the blends of SP-15 (showed by arrows) and SP-20. It is indicative of thermodynamically immiscible blends, which has been confirmed by thermal analysis. However, the blends show good interfacial adhesion between PU and TPS phases. This maybe due to the hydrogen bonding interactions between the urethane groups of PU and the hydroxyl groups on starch. These interactions lead to lowering the interfacial tension between PU and TPS phases, leading to compatibilization [10].

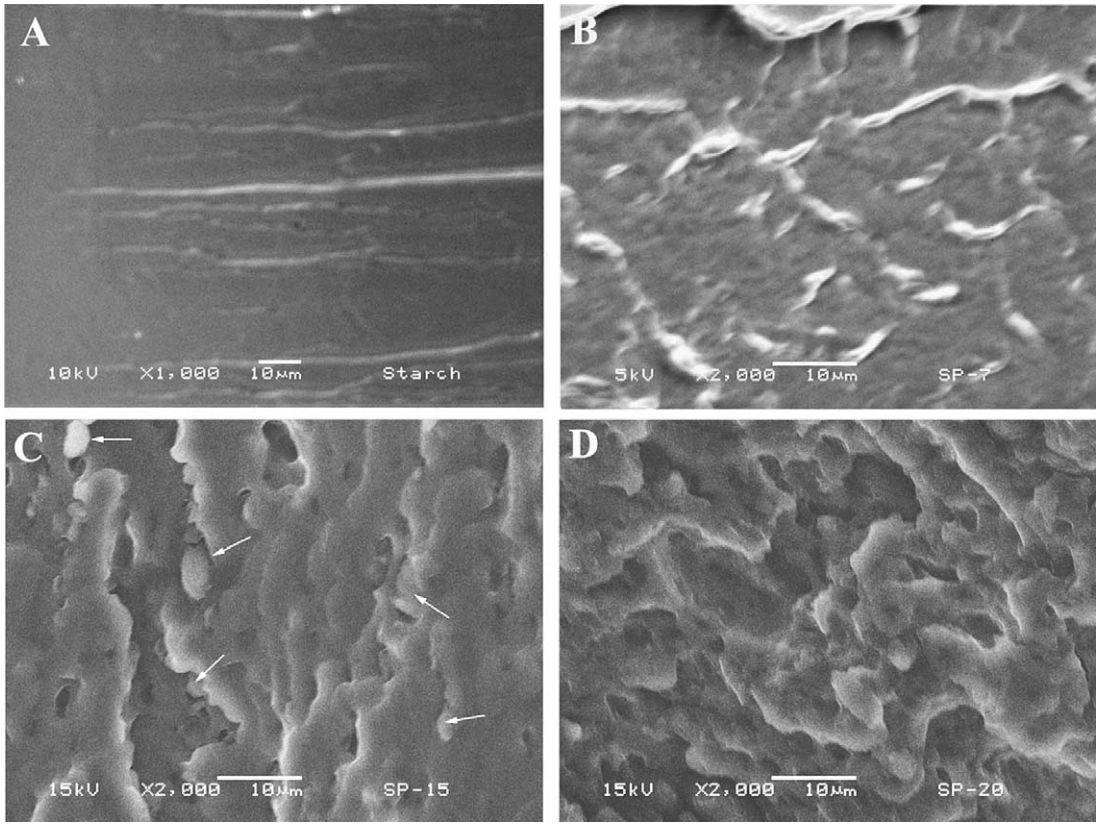

Fig. 5. SEM images of TPS (A), SP-7 (B), SP-15 (C) and SP-20 (D).

3.2. Mechanical properties

Table 2 shows the mechanical properties of the blends after aging 2 and 30 weeks at 52% RH. The castor oil PU shows the characteristic of ductile polymers (not shown). The Young's modulus, tensile strength and elongation at break are 44.5±3.8 MPa, 11.8±2.1 MPa and 279±11.2%, respectively. The values of tensile strength and elongation at break of TPS are similar to that with similar formulation reported elsewhere [34]. For the blends, the tensile strength first increases with increasing PU content and reaches its maximum (5.1 MPa) at 15 wt% content of PU, then decreases to 2.6 MPa at 30 wt% PU. Simultaneously, the elongation at break increases from 120 to 176% with increasing PU content from 0 to 10 wt%, and then slightly decreases with further increasing PU content from 15 to 30 wt%. This indicates that incorporating appropriate content of PU into TPS matrix can improve the mechanical properties in both tensile strength and elongation at break of the blends. When PU content is higher than 15 wt %, the resulting blends exhibit a decrease in tensile strength and elongation at break, due to some phase separation as proved by DSC, DMTA and SEM. The mechanical behavior of TPS/PU blends is different from that of the blends of both TPS/PCL [34] and TPS/PLA [35], whose elongation at break significantly decreases when PCL or PLA is added. The mechanical property evolution during aging is also presented in Table 2. After aging of 30 weeks, a much increase in both Young's modulus and tensile strength is observed for TPS and blends compared with the non-aged ones. This can be attributed to the retrogradation of starch during the storage, because crystallinity development is well known to increase the mechanical properties and more specifically the Young's modulus and stress [36]. It is worth noting that the blends with 4–15 wt% PU still exhibit relative high flexibility expressed by elongation at break (92–121%). Fig. 6 shows the stress–strain curves of TPS and blends conditioned for 2 and 30 weeks. These curves clearly show a typical characteristic of ductile polymers. The blends exhibit two characteristic regions of deformation behavior in their tensile stress–strain curves. At low strains (<10%) the stress increased rapidly with a slight increase in the strain. The initial slopes were steep in the elastic region, indicating the relatively high elastic moduli of these novel blends. At high strain (>10%) the blends show a slow increase in stress with strain until failure occurs. The stress–strain curve gives not only the modulus and strength indications of the material, but also its toughness. The toughness of TPS/PU blends, obtained from area under the corresponding tensile stress–strain curve, is also summarized in Table 2. The toughness exhibits a trend similar to tensile strength, indicating that determination of the toughness is significantly influenced by the tensile strength. The maximum toughness can be, respectively, seen for the blends SP-10 (aged 2 weeks) and SP-7 (aged 30 weeks), showing the best energy absorption capability compared with the other blends. From the results mentioned above, it is obviously that PU plays an important role in enhancing the tensile strength, elongation at break and toughness of the blends.

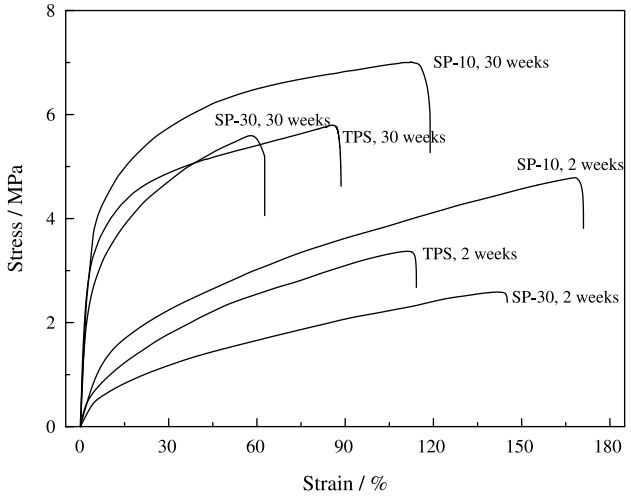

Fig. 6. The stress–strain curves of TPS and TPS/PU blends aged for 2 and 30 weeks, respectively.

3.3. Surface properties and water absorption

Fig. 7 shows effect of PU content on the contact angle values of TPS/PU blends at room temperature. The TPS has a lower contact angle of 34.4°, and the angle decreases rapidly after water droplet deposition. The water droplet is

Table 2
Mechanical properties of the TPS, PU and TPS/PU blends: Young's modulus (E), tensile strength (σ_b), toughness (T) and elongation at break (ε_b)

Films	Aging times: 2 weeks				Aging times: 30 weeks			
	E (MPa)	σ_b (MPa)	T (MPa)	ε_b (%)	E (MPa)	σ_b (MPa)	T (MPa)	ε_b (%)
TPS	40.3±5.1	3.4±0.3	2.6±0.3	116±9.2	88.6±6.3	5.8±0.3	4.4±0.5	88±5.8
SP-4	58.6±3.2	3.9±0.2	3.7±0.3	120±6.5	102.8±4.5	8.6±0.3	7.4±0.7	106±8.2
SP-7	74.5±6.9	4.6±0.4	4.5±0.2	138±7.3	125.5±8.2	8.8±0.3	7.9±0.6	97±7.6
SP-10	67.7±7.2	4.9±0.3	5.2±0.3	176±8.4	130.1±6.4	7.2±0.4	7.2±0.7	121±4.5
SP-15	43.3±6.4	5.1±0.4	5.1±0.3	158±6.8	153.9±9.2	6.5±0.2	5.4±0.5	92±4.3
SP-20	35.2±5.6	3.4±0.2	3.5±0.2	145±7.7	163.0±7.8	6.3±0.4	3.4±0.4	66±6.1
SP-30	27.4±2.7	2.6±0.3	2.5±0.2	143±5.1	107.3±5.4	5.5±0.3	2.9±0.3	64±2.5
PU	44.5±3.8	11.8±2	14.9±2.1	279±11.2	–	–		–

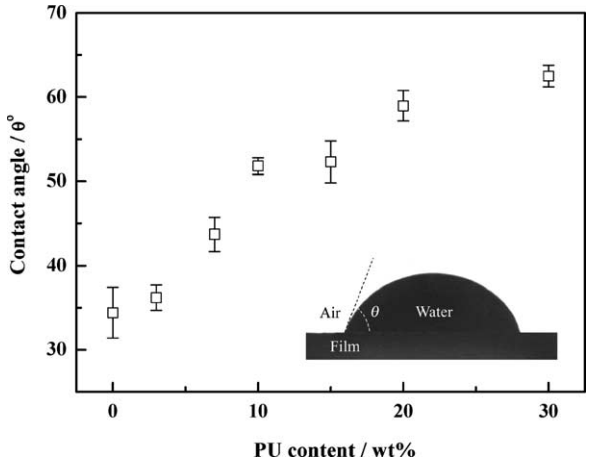

Fig. 7. Dependence of contact angle of TPS/PU blends on PU content.

totally absorbed by TPS films within about 30 s. This behavior indicates the hydrophilic and highly wettable characteristics of TPS surface. When PU is blended with TPS, the contact angle value of the blends increases significantly from 34.4 to about 63°. Moreover, the evolution of contact angle with time slows down. This indicates that both the hydrophobic PU and the lower glycerol content might be responsible for the improvement of hydrophobic characteristic of the resulting blends [37].

The equilibrium water uptake of the TPS/PU blends as a function of PU content is shown in Fig. 8. It is observed that TPS absorbs about 69% water. The dashed line is the theoretical values of equilibrium water uptake, $WU_{(theory)}$, obtained from the additivity rule as the following equation:

$$WU_{(theory)} = w_{TPS}WU_{TPS} + w_{PU}WU_{PU}$$

where WU and w are, respectively, the equilibrium water uptake and mass fraction in the blends. Comparing with the theoretical values, a relatively low water uptake value is observed for the blends, indicating that some morphology differences of those hydrogen bonded blends with that of the physical blends. The water uptake of the blends decreases non-linearly from 64 to 52 wt% with increasing PU content from 4 to 15 wt%. This behavior suggests occurrence of strong hydrogen bonding interaction between PU and TPS. This interaction tends to stabilize and prevents the swelling of the TPS matrix in high moisture environment, leading to a reduction of the water absorption. This is in good agreement with the results from DSC, DMTA. However, the water uptake values of SP-20 and SP-30 are parallel to the reference calculated by additivity rule, implying that equilibrium water uptakes of TPS/PU blends are less affected by addition of PU. This behavior can, to some extent, support the occurrence of phase separation in the resulting blends.

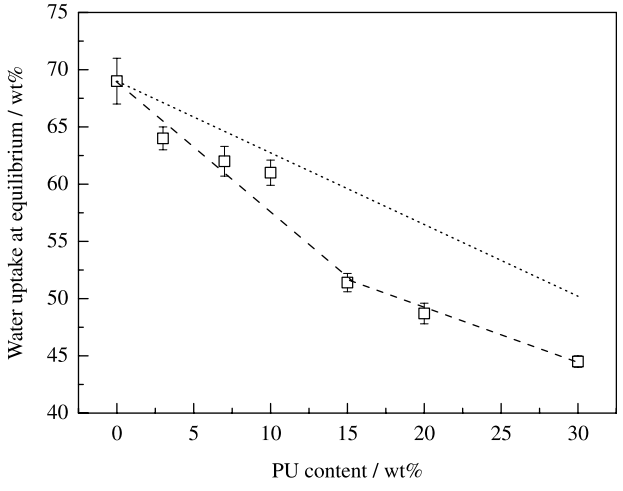

Fig. 8. Dependence of water uptake at equilibrium on PU content for TPS/PU blends.

4. Conclusions

In this work, we prepared a novel PU dispersion from natural occurring castor oil, and then used the PU dispersion to blend with thermoplastic starch (TPS) for preparation of the new biodegradable bio-plastics by extrusion. Compared with TPS, the TPS/PU blends exhibit the improved physical properties. The good or partial miscibility occurs between TPS and PU due to the hydrogen bonding interaction between urethane groups of PU and hydroxyls on starch. The interaction leads to an increase in Young's modulus (40–75 MPa), tensile strength (3.4–5.1 MPa), elongation at break (116–176%) and toughness (2.6–5.2 MPa). Further, even aged for 30 weeks, these blends still exhibit relative high values of the elongation at break of about 64–120%. In addition, the TPS/PU blends also show the surface and bulk-hydrophobicity and an increase in water-resistance due to incorporation of castor oil based waterborne polyurethane.

This work provides a new way to overcome the most important weaknesses of poor resilience and moisture sensitivity for TPS by blending a novel polymer based on renewable resources. It is an interesting approach to produce low cost biodegradable plastics in order, for instance, to increase the use of environmentally friendly materials in packaging.

Acknowledgements

This work is supported by Conseil Régional de Champagne-Ardenne, Conseil Général de la Marne, and la Ville de Reims through a research program devoted to the development of new biodegradable packaging materials based on starch. The authors are indebted to Dider Ranchon and Alain Lemaitre for their technical help.

References

[1] Mohanty AK, Misra M, Hinrichsen G. Macromol Mater Eng 2000; 276/277:1–26.
[2] Lu YS, Weng LH, Zhang LN. Biomacromolecules 2004;5:1046–51.
[3] Choi EJ, Kim CH, Park JK. J Polym Sci, Part B: Polym Phys 1999;37: 2430–8.
[4] Dufresne A, Vignon MR. Macromolecules 1998;31:2693–6.
[5] Suvorova AI, Tyukova IS, Trufanova EI. Russ Chem Rev 2000;69: 451–9.
[6] Ratto JA, Stenhouse PJ, Auerbach M, Mitchell J, Farrell R. Polymer 1999;40:6777–88.
[7] Carvalho AJF, Job AE, Alves N, Curvelo AAS, Gandini A. Carbohydr Polym 2003;53:95–9.
[8] Guan JJ, Hanna MA. Biomacromolecules 2004;5:2329–39.
[9] Guan JJ, Hannan MA. Ind Crops Prod 2004;19:255–69.
[10] Shin B-Y, Lee S-I, Shin Y-S, Balakrishnan S, Narayan R. Polym Eng Sci 2004;44:1429–38.
[11] Rouilly A, Rigal L, Gilbert RG. Polymer 2004;45:7813–20.
[12] Zhang JF, Sun X. Biomacromolecules 2004;5:1446–51.
[13] Wang H, Sun X, Seib P. J Appl Polym Sci 2002;84:1257–62.
[14] Wollerdorfer M, Bader H. Ind Crops Prod 1998;8:105–12.
[15] Anglès MN, Dufresne A. Macromolecules 2000;33:8344–53.
[16] Anglès MN, Dufresne A. Macromolecules 2001;34:2921–31.
[17] Wilhelm H-M, Sierakowski M-R, Souza GP, Wypych F. Carbohydr Polym 2003;52:101–10.
[18] Huang MF, Yu JG, Ma XF. Polymer 2004;45:7017–23.
[19] Lu QW, Macosko CW. Polymer 2004;45:1981–91.
[20] Yoon PJ, Han CD. Macromolecules 2000;33:2171–83.
[21] Nobel KL. Prog Org Coat 1997;32:131–6.
[22] Delpecha MC, Coutinho FMB. Polym Test 2000;19:939–52.
[23] Ha S-K, Broecker HC. Polymer 2002;43:5227–34.
[24] Cao XD, Zhang LN, Huang J, Yang G, Wang YX. J Appl Polym Sci 2003;90:3325–32.
[25] Lourdin D, Coignard L, Bizot H, Colonna P. Polymer 1997;38: 5401–6.
[26] Sormana J-L, Meredith JC. Macromolecules 2004;37:2186–95.
[27] Biliaderis CG, Lazaridou A, Arvanitoyannis I. Carbohydr Polym 1999;40:29–47.
[28] Bikiaris D, Prinos J, Botev M, Betchev C, Panayiotou C. J Appl Polym Sci 2004;93:726–35.
[29] Brannock GR, Barlow JW, Paul DR. J Polym Sci, Part B: Polym Phys 1991;29:413–29.
[30] Chung HJ, Woo KS, Lim ST. Carbohydr Polym 2004;55:9–15.
[31] Demirgöz D, Elvira C, Mano JF, Cunha AM, Piskin E, Reis RL. Polym Degrad Stab 2000;70:161–70.
[32] Lourdin D, Bizot H, Colonna P. J Appl Polym Sci 1997;63:1047–53.
[33] Martin DJ, Meijs GF, Renwick GM, Gunatillake PA, McCarthy SJ. J Appl Polym Sci 1996;60:557–71.
[34] Averous L, Moro L, Dole P, Fringant C. Polymer 2000;41:4157–67.
[35] Martin O, Averous L. Polymer 2001;42:6209–19.
[36] Delville J, Joly C, Dole P, Bliard C. Carbohydr Polym 2003;53: 373–81.
[37] Lepifre S, Froment M, Cazaux F, Houot S, Lourdin D, Coqueret X, et al. Biomacromolecules 2004;5:1678–86.